PREPRINT

PERTANIKA JOURNALS

SCIENCE & TECHNOLOGY

Journal homepage: http://www.pertanika.upm.edu.my/

Effects of NaOH Concentration and Plate Surface Texture on the Performance of the HHO Generator

Asmawi Marullah Ridwan[1,2], Muhd Ridzuan Mansor[1]*, Noreffendy Tamaldin[1], Fahamsyah Hamdan Latief[2] and Viktor Vekky Ronald Repi[3]

[1]*Faculty of Mechanical Technology and Engineering, Universiti Teknikal Malaysia Melaka, Hang Tuah Jaya, Durian Tunggal 76100, Melaka, Malaysia*

[2]*Department of Mechanical Engineering, Faculty of Engineering and Science, Universitas Nasional, Jakarta 12520, Indonesia*

[3]*Department of Engineering Physics, Faculty of Engineering and Science, Universitas Nasional, Jakarta 12520, Indonesia*

ABSTRACT

The need for clean energy as an alternative is inevitable. HHO gas has received much attention lately. In addition to electrolyte concentration, the breakthrough with a diverse electrode surface texture approach has not been extensively performed. Therefore, this study aims to determine the effects of NaOH concentration and plate surface texture on the performance of the HHO generator. In general, the increase in electrolyte concentration combined with surface texture caused an increase in output current, HHO gas production, and output temperature. As for the applied voltage variation with various surface textures, the increase in output current, HHO gas production, and output temperature also took place, similar to the case of increasing NaOH concentration. Either an increase in electrolyte concentration or an increase in applied voltage triggers faster ion movement, leading to an increase in conductivity, thus effectively assisting the electrolysis of water. Regarding the output current and HHO gas production, the textured surface had a much higher value than the plain surface in terms of increasing NaOH concentration or applied voltage variations. However, according to the R^2 results, the linear surface has a stronger relationship with the output current and HHO gas production than the cross surface. In the case of the output temperature, the linear surface was slightly lower than the

ARTICLE INFO

Article history:
Received: 19 July 2023
Accepted: 20 November 2023
Published: 01 April 2024

DOI: https://doi.org/10.47836/pjst.32.3.08

E-mail addresses:
asmawi@civitas.unas.ac.id (Asmawi Marullah Ridwan)
muhd.ridzuan@utem.edu.my (Muhd Ridzuan Mansor)
noreffendy@utem.edu.my (Noreffendy Tamaldin)
fhlatief@civitas.unas.ac.id (Fahamsyah Hamdan Latief)
vekky_repi@civitas.unas.ac.id (Viktor Vekky Ronald Repi)
* Corresponding author

ISSN: 0128-7680
e-ISSN: 2231-8526

cross surface. It is possibly due to impurities in the electrolyte solution that contaminate the electrode surface, resulting in a lower output temperature on the linear surface.

Keywords: HHO generator, hydrogen, NaOH, performance, surface texture

INTRODUCTION

The ongoing problem of global warming and ozone layer depletion has prompted a search for renewable energy alternatives that do not emit harmful pollutants to human health and the environment. In addition, this is also inspired by the availability of fossil fuels that have begun to deplete; thus, the development and discovery of renewable energy must get more serious attention for the benefit of human life in the future (Dufour et al., 2011; Muritala et al., 2020). One alternative energy introduced lately through the development of oxyhydrogen (HHO) generators has an economic advantage and a main resource easily obtained and available in nature, namely water (Dincer & Zamfirescu, 2012).

Among the various types of alternative fuels that exist, hydrogen gas is the cleanest energy source. The hydrogen gas can be principally produced using electrolysis (Grigoriev et al., 2020), which is achieved by separating the atoms contained in water molecules by applying electric current to the cathode and anode, acting as negative and positive poles, respectively, immersed in water, resulting in chemical reactions in accordance with the concept of redox. The interesting things about HHO gas are its lightness, colourlessness, easy reaction with other chemicals, and flammability. However, the improvements in the performance of the generator are still needed. The proposed method to improve its performance is either increasing the concentration of the catalyst, which is made of an electrolyte solution (Hassan et al., 2022; Soler et al., 2009), or, more recently, manipulating the effective surface of the electrode plate (Ayub et al., 2022).

Meanwhile, surface texture engineering has been introduced in recent years to optimise engine performance and is expected to expand its practical applications (Rao et al., 2021). For example, in a study conducted by Borghi et al. (2008), the effect of surface modification by laser texturing on the tribological performance of nitrided steels for high-performance engine applications was thoroughly investigated. The original idea of surface texture engineering was to improve the mechanical and tribological properties of engine metal components (Naat et al., 2023; Rajput et al., 2021). It is noted that the chemical composition and surface hardness of objects have an important influence on the wear resistance of materials under sliding conditions. Many components made of steel or other ferrous materials are nitrided to improve their wear resistance, fatigue strength, and corrosion resistance (Fahy, 2014; Kato et al., 1994). Moreover, surface texture fabrication has been carried out by various techniques, i.e., chemical etching, atomic layer deposition, ultrasonic-assisted milling, laser surface texturing, micro-milling, and electrical discharge

(EDM) (Ayub et al., 2022; Li et al., 2018; Li et al., 2022). Based on the literature review, surface texture engineering provides several advantages, including lowering friction and wear, increasing load-carrying capacity, and increasing fluid layer stiffness. Previous studies hinted that the surface texture of the electrode impacts electrolysis, which in turn impacts the rate of hydrogen gas production (Xu et al., 2021; Zeng & Zhang, 2014).

An equally important variable for increasing hydrogen gas production is the type of electrolyte solution and concentration levels used. Among the types of electrolytes that have been used previously in HHO generators are potassium hydroxide (KOH) (Karthik, 2017; Manu et al., 2016) and sodium hydroxide (NaOH) (Alam & Pandey, 2017; Ismail et al., 2018). Many studies have been conducted to find the relationship between the electrolyte type and the HHO gas production rate. The results show that the electrolyte concentration is important in increasing the HHO gas flow rate. It was also found that an increase in electrolyte concentration by 1% molality led to increased current consumption (Yilmaz et al., 2010). Fiala et al. (2013) have conducted a comparative study on the use of KOH and NaOH in HHO generators. The conclusion obtained is that the use of a KOH electrolyte concentration of 10% was able to achieve optimal conditions because KOH has better chemical stability and more efficient HHO gas production when compared to NaOH. Santilli (2006) reported that sulfuric acid and other electrolytes are sometimes added to KOH and NaOH to promote water electrolysis.

Apart from what has been described above, it turns out that other important parameters also affect the production of HHO gas, such as the cross-sectional area of the electrodes used, the distance between electrodes, the configuration of the plate arrangement, and the type of electrode plate materials, (Ridhuan et al., 2021). With regard to the lack of research on the effect of surface texture on electrode plates that have been carried out, the combination of the two variables, in this case, the type of electrolyte and the surface texture of the electrode, is a very interesting and promising topic for further study in efforts to develop HHO generators in the future. Therefore, the main objective of this study is to evaluate the effects of varying NaOH concentrations and the surface texture of the electrode plates on the performance of the HHO generator.

MATERIALS AND METHODS

Materials

In this study, the first stage involves modifying the surface of the electrode plate to be installed on the HHO generator. Following the modification, performance testing of the HHO generator was conducted with variations in NaOH catalyst concentrations, specifically 10 g, 20 g, 30 g, 40 g, 50 g, and 60 g, respectively, at 12V applied voltage. Subsequently, the applied voltage was kept constant at 12V for all test parameters. The research then proceeded to test the performance of the HHO generator using electrode cell plates with

different surface textures. These surface textures of the electrode plate consist of plain, linear, and cross patterns (Figure 1). The output parameters analysed based on the catalyst concentration and application voltage input include the HHO gas production rate, output current, and output temperature.

The electrode plate base material is made of commercial 316 stainless steel labelled "SS316L," which has a chemical composition as shown in Table 1. The electrode plates used in this study have dimensions of 100 mm × 100 mm × 1 mm and three different types of plate surface textures, as illustrated in Figure 1. Based on the prepared design, the HHO generator was equipped with five SS316L electrode plates with 2 mm between each plate.

Table 1
The chemical composition of SS316L (in wt.%)

Fe	Cr	Ni	Mo	Mn	C	P	S	Si	N
Bal.	16	10	2	2	0.03	0.045	0.03	0.75	0.1

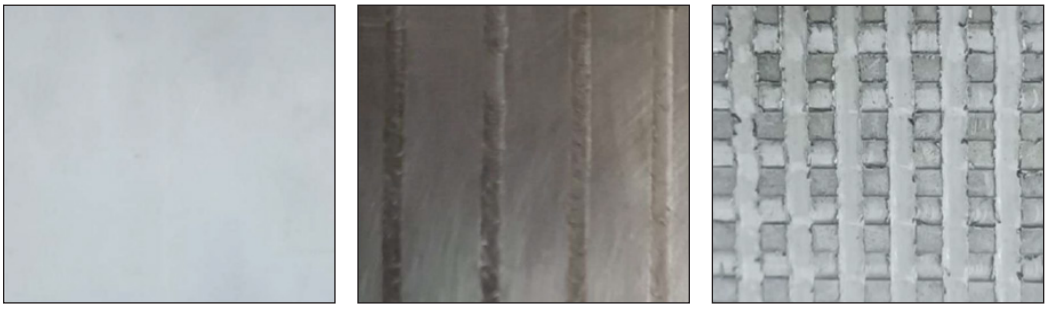

(a) (b) (c)

Figure 1. Surface texture types of electrode plates used in HHO generators: (a) plain; (b) linear; and (c) cross-surface

Fabrication of Electrode Surface Textures

The texturing of the electrode surface was performed using a machining process. The first step starts with creating patterns for each design using CAD software called CATIA V5 R20 to produce patterns with good precision and accuracy, as presented in Figures 2 and 3. The second step is to use the patterns prepared to proceed with the machining process and obtain the program codes for each pattern. In the third step, the program codes were input into the CNC machine to create the desired texture on the surface of each electrode plate. Electrode surface texturing was performed using a machining process. The first step was to create patterns for each design using CAD software, CATIA V5 R20, to produce patterns with precision and accuracy. In the second step, based on the created patterns, the machining process was continued to obtain the program codes for each pattern. In the third step, the program codes are input into the CNC machine to create the desired texture on the

surface of each electrode plate. In the fourth step, the fabrication process for texturing was carried out at 1150 mm/min for about 20 minutes for each type of plate. In the fifth step, coolant was continuously applied during the machining process to lubricate the contact area between the surface of the plate and the tool and to cool the temperature arising from

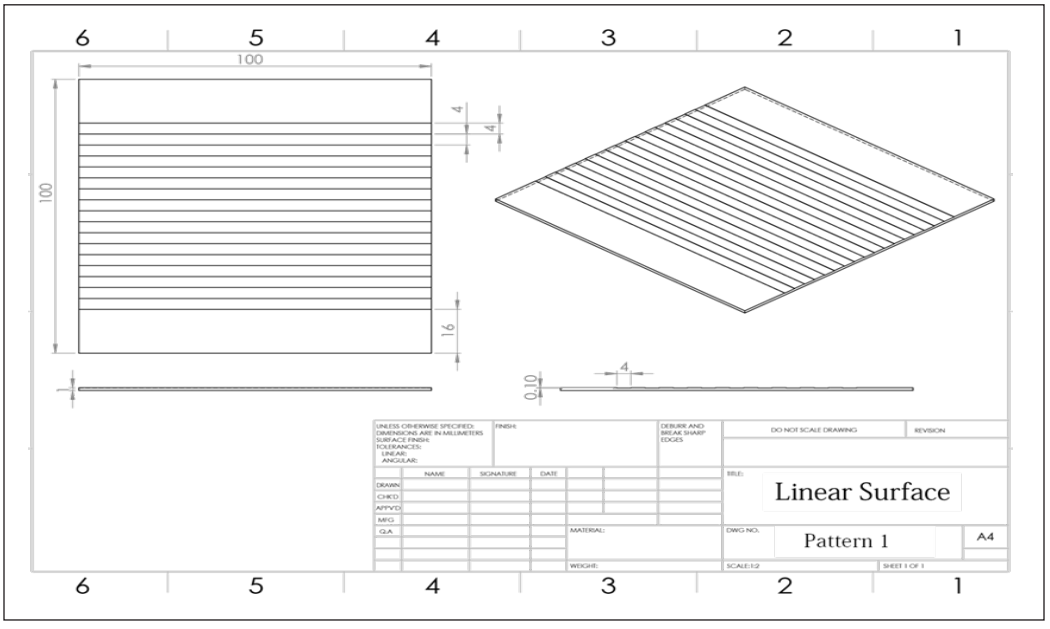

Figure 2. The surface texture design of the electrode plate with a linear pattern (unit dimension = mm)

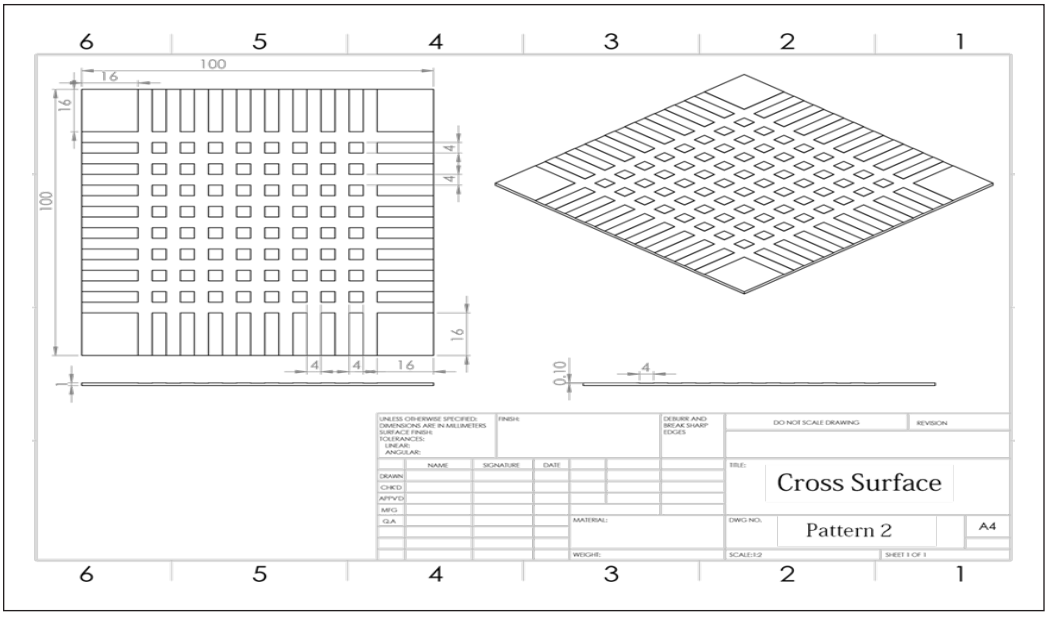

Figure 3. The surface texture design of the electrode plate with a cross-pattern (unit dimension = mm)

the contact, thus preventing tool wear and producing a good surface finish. The last step was to ensure that the surface of the electrode plate was free from any remaining cutting residue with the aid of a tool file before polishing with isopropyl.

Setup of the HHO Generator

In this study, the designed HHO generator combines wet cells and dry cells since both cell types have advantages over each other that are interesting to observe. It should be noted that the calibration method was used to assess the performance of the HHO generator in producing the desired HHO gas. A detailed schematic of the HHO generator parts is shown in Figure 4. The following steps need to be taken to set up the HHO generator: NaOH electrolyte solution is put into the container to submerge the electrode plates completely. Then, the power supply is connected to the HHO generator by providing a constant input voltage of 12 V. After the voltage is supplied, the electrolysis process takes place, and bubbles begin to appear slowly as a sign of HHO gas production. The calibration method is used to evaluate the performance of the HHO generator in producing the HHO gas.

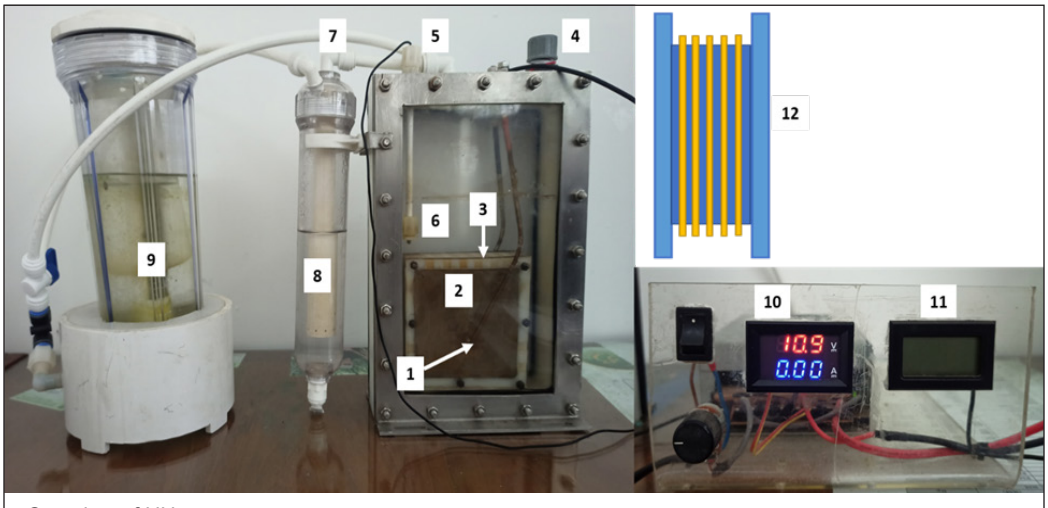

Overview of HHo generator parts:

1. Electric power rod
2. Spacer module
3. Electrode plates arrangement
4. Water inlet
5. HHO gas outlet
6. Thermocouple
7. HHO gas flow pipe
8. Bubbler tube
9. Flowmeter
10. Voltmeter and Amperemeter
11. Thermometer
12. Enlargement of no.3

Figure 4. Schematic arrangement of the parts of the HHO generator

Measurement Procedures

The procedure of measuring the output current, HHO gas production rate, output temperature, and operating time is important to understand. Systematically, it starts filling the container with NaOH electrolyte with a predetermined concentration ranging from 10

g/L to 60 g/L so that the installed electrode plates are thoroughly and evenly submerged. Then, the "on" button on the generator is pressed to activate the electricity needed for the electrolysis process to take place as expected. After pressing the on button, the HHO generator is allowed to stand for approximately 30 minutes to stabilise its condition. After a stable condition has been achieved, the voltage is kept constant at 12 V, and the stopwatch starts to be activated at the beginning of the calculation.

Furthermore, the HHO gas production process runs as the operating time increases, which causes a gradual increase in the volume of water in the flowmeter so that the scale shows a value of 10 ml (assumed to be the maximum value), which indicates that the hydrogen production rate is running well and is usually followed by an increase in temperature due to the chemical reactions taking place. After reaching the maximum condition, the HHO generator engine was immediately deactivated, the amount of output current produced was visible on the power supply screen, the volume of hydrogen gas produced was easily identified, and the output temperature was also read on the screen via the thermocouple connection connected to the generator. The operating time is calculated from the start of the generator being turned on until it is turned off, which can be read through a stopwatch. The results of each determined parameter are obtained from the various observations made. In the final stage, data analysis is needed to be able to find out how variations in NaOH electrolyte concentration and electrode plate surface texture affect the actual performance of the HHO generator.

RESULTS AND DISCUSSION

Effect of NaOH Concentration on Output Current at Varying Plate Surface Textures

Figure 5 shows the relationship between the output current and NaOH concentration at various surface textures of the electrode plate under the condition of a constant voltage of 12 V. It is obviously seen that the output current increases with increasing NaOH concentrations from 10 g/L to 60 g/L, which occurs in all types of plate surface textures. From the results obtained, increasing the electrolyte concentration plays an important role in producing the output current obtained. It is understandable that the NaOH electrolyte will decompose into Na+ and OH- ions, resulting in electron

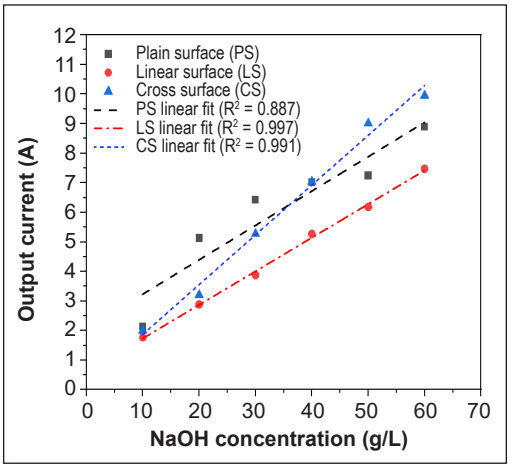

Figure 5. Output current vs. NaOH concentration under varying plate surface textures at 12V applied voltage

transfer and increased water conductivity (Rusdianasari et al., 2019). Increasing the electrolyte concentration has an impact on increasing the rate of electron transfer between the installed electrode plates.

Even further, the conductance generated by the electrodes also increased. Because of these two things, the output current achieved will vary, and if observed carefully, it comes down to the rate of water dissociation (Wang et al., 2021). In contrast, increasing electrolyte concentration decreases the electrical resistance and increases the current. On the other hand, decreasing electrolyte resistance can cause an increase in electrical conductivity and a decrease in potential simultaneously. Besides that, the resistance in the electrolyte and electrodes can affect the resulting current output values due to side reactions, inverse reactions, and the factor of impurities attached to the electrode surface. The impurities in the electrolyte, such as magnesium, calcium, and chloride ions, can also cause side reactions. On the other hand, the resistances in the electrolytic solution and electrodes brought on by inverse reactions, side reactions, and impurities in electrode material also influence the electric current values obtained (Zeng & Zhang, 2010).

Another reason to consider is the distance between the electrode plates. In this study, the distance between the electrodes was 2 mm, indicating a much closer distance between the electrodes. As mentioned in the previous study, close spacing between electrodes effectively reduces the electrical resistance between the electrodes, increasing the amount of current generated (Galama et al., 2016). Still related to Figure 5, the increase in output current at electrolyte concentrations of 10 g/L to 60 g/L is above 300% for all electrode surface textures. However, from a linear regression perspective, the highest R^2 value is for the linear surface texture of 0.997, which means the accuracy is very good for this linear surface. The results also indicated that using different electrode surface texture types affects the output current achieved by the HHO generator. The surface textures created make a difference in the effective surface area of the electrodes. The surface area calculation of each surface texture is summarised in Table 2.

Table 2 shows that the cross-sectional area for the linear surface is 101.8 cm^2, which is the highest compared to the other types. The relationship between electrode cross-sectional area and electrical resistance is given in Equation 1 (Mazloomi & Sulaiman, 2012).

$$R = \frac{\rho\, l}{A} \quad (1)$$

where R is the electrical resistance of the material, ρ is the electrode material's resistivity, A is the cross-sectional area of the electrode and l is the distance between the electrodes used to do the measurement. The

Table 2
Cross-section area of the electrode plate with varying surface textures

Type of surface textures	Texture labelling	Cross-section area (cm^2)
Plain surface	PS	100.00
Linear surface	LS	101.80
Cross surface	CS	102.30

large cross-sectional area allows the resulting electrical resistance to be small. It is known that electrical resistance is the opposite of electric current; thus, when electrical resistance decreases, the resulting output current will increase. It is also necessary to understand that the surface area of the electrode plate refers to the area of the conducting plate, which functions to transmit electric current. The broader the cross-section area, the greater the electric current that can be delivered (Poimenidis et al., 2021).

Effect of NaOH Concentration on HHO Production Rate at Varying Plate Surface Textures

Figure 6 illustrates the HHO gas production rate against the NaOH electrolyte concentration at different electrode surface textures. Similar to the output current, the same trend is also shown by the HHO gas production rate, where the increase fully influences the increase in HHO gas production in electrolyte concentration. The results showed that the increase in HHO gas production rate was above 200% for all electrode surface textures. As for the 60 g/L electrolyte concentration, the HHO gas production rate value is 305.93 L/min, 291.09 L/min, and 218.08 L/min for cross, linear, and plain surface textures, respectively. It should be noted that increasing the electrolyte concentration can generally accelerate the movement of molecules in the water so that a higher-intensity collision process occurs between molecules available in it, such as hydrogen and oxygen. The higher the intensity of collisions between molecules in the water, the greater the amount of HHO gas produced (El Soly et al., 2021). However, based on the statistical approach, the linear surface texture had the highest R^2 value of 0.991. In addition to the increase in electrolyte concentration, it appears that the difference in electrode surface texture has a positive impact on the rate of HHO gas production. Texturing the surface of the electrode plates has affected their surface roughness, which results in a difference in cross-sectional area between each other. The results obtained align with the achievements Fahy reported (2014).

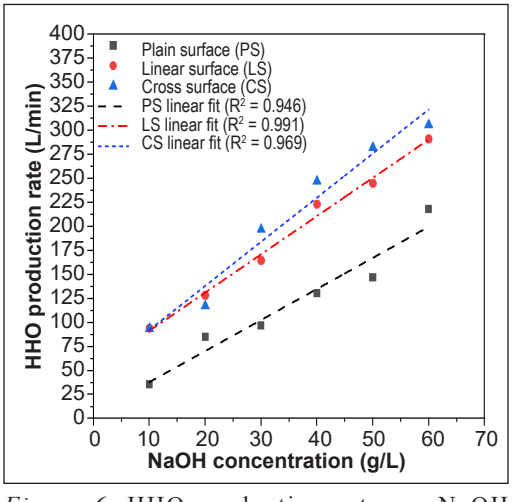

Figure 6. HHO production rate vs. NaOH concentration under varying plate surface textures at 12 V applied voltage

Another important factor is the type of electrode plate material. This study used SS316L, which has a high nickel concentration (about 10 per cent by weight), as the electrode. The electrode made of SS316L is in an alkaline environment because it uses NaOH as the electrolyte, where the hydrogen evolution reaction (HER) takes place at the cathode, which acts

as the negative pole. In contrast, at the anode, which acts as the positive pole, the oxygen formation reaction (OER) takes place. As a function of time, the hydrogen evolution rate (HER) increases with rising electrolyte concentration. However, the HER rate tends to be slower in NaOH compared to KOH. The characteristics of the electrocatalytic surface significantly influence the HER rate. Electrochemical analysis of stainless steel indicates that 316 steel is the optimal choice for a cathodic electrode in inducing HER within the solution.

The HER rate is not only affected by the concentration of the electrolyte but also impacts the formation of metal hydrides in stainless steel, minimising corrosive effects on the material. Meanwhile, oxygen hydroxide (OH) originates from the water structure and surfaces of OER. The presence of OH serves a dual purpose: firstly, an excess of OH can detrimentally affect conductivity and structural integrity. Secondly, moderate OH levels with the right level of acidity at the electrode/electrolyte interface can positively influence the fundamental oxygen evolution reaction and thermodynamically reduce the ion release rate. It is based on the non-electrocatalytic activity in oxygen evolution reactions, as well as the identification of crystalline defects and stoichiometric oxide anode levels, which contribute to the oxygen evolution reactions.

Of course, this phenomenon is most likely inseparable from the formation of the nickel hydrate layer, which acts as a protective layer on the electrode surface, allowing the corrosion rate to be suppressed, which results in a fairly high HHO gas production rate (Olivares-Ramírez et al., 2007). The minimum corrosion effect greatly contributes to the smoothness of the hydrogen formation reaction (Vračar & Conway, 1990). Coupled with surface texture engineering, this will be a promising technique and should be taken into account for the development of further enhancements of HHO gas production. The details of the chemical reaction Equations 2, 3 and 4 at each pole are shown as follows gas (Subramanian & Thangavel, 2020):

$$\text{Reaction at the cathode: } 2\,H_2O\,(l) + 2e^- \rightarrow H_2\,(g) + 2\,OH^-\,(aq) \quad (2)$$

$$\text{Reaction at the anode: } 4\,OH^-\,(aq) \rightarrow O_2\,(g) + 2\,H_2O\,(l) + 4\,e^- \quad (3)$$

$$\text{Overall reaction: } 2\,H_2O\,(l) \rightarrow 2\,H_2\,(g) + O_2\,(g) \quad (4)$$

According to stoichiometry, the above chemical reaction shows that the production of hydrogen gas is double that of oxygen gas (Subramanian & Thangavel, 2020).

Effect of NaOH Concentration on Output Temperature at Varying Plate Surface Textures

The results of the output temperature versus NaOH concentration at different surface textures are shown in Figure 7. The output temperature generally shows an increasing trend

with increasing NaOH concentration at all types of electrode surface textures, where the temperature increase ranges above 40 per cent for NaOH electrolyte concentrations of 0–60 g/L. The final output temperatures at 60 g/L concentration were 42.5°C for the plain surface, 45.13°C for the linear surface, and 46.55°C for the cross surface. However, there was some temperature instability for each type of surface texture. The most obvious instability is for the electrode with cross-surface texture, where there is a decrease in the output temperature at two different concentrations, one from 39.05°C to 24°C and the other from 50.18°C to 46.55°C.

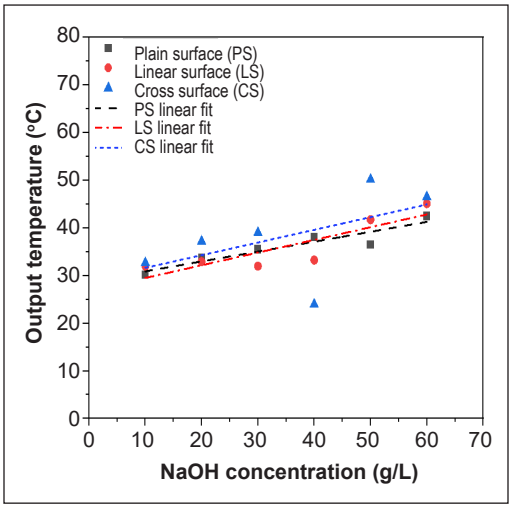

Figure 7. Output temperature vs. NaOH concentration under varying plate surface textures at 12 V applied voltage

This instability phenomenon may be due to the type of electrolyte used, NaOH. The basic principle of an electrolyte solution is that it is influenced by the mobility and conductivity of ions that decompose in the solution. As already stated, the mobility and conductivity of Na+ ions are lower than those of K+ ions (Cao et al., 2009). It is likely to cause instability in the resulting output temperature, and the presence of impurities in the electrolyte solution that could contaminate the electrode surface must also be considered (Doche et al., 1999).

The type of electrolyte and electrolyte concentration play an important role in water electrolysis. NaOH is strong as a type of electrolyte; it decomposes completely into ions when dissolved in water, so it has a fairly high conductivity. When the electrolyte concentration is increased, it increases the intensity of collisions between ions, making them more intense. The resulting impact is increased conductivity, accompanied by higher ion mobility during the water electrolysis process. Due to the increased conductivity, it produces an electrolyte solution temperature that is much hotter than its initial condition, and thus, the output temperature of the HHO generator also rises (Sun & Hsiau, 2018; Yuvaraj & Santhanaraj, 2014).

Effect of Applied Voltage on Output Current at Varying Plate Surface Textures

Figure 8 shows the applied voltage and output current at varying electrode surface textures. Their relationship shows good linearity, where the output current increases with increasing input current. Upon further observation, the increase in output temperature is more prominent on textured electrode surfaces, with an increase of over 300% on both types

of textured electrode surfaces. In contrast, the increase in output current is only about 148% for plain surfaces with increasing applied voltage. Beyond that, the largest R^2 value of 0.982 was experienced by the electrode with a linear surface. This value indicates a strong relationship between the input voltage variation and the output current.

Figure 8 shows that a higher applied input voltage will accelerate the decomposition reaction in water electrolysis. The supplied applied voltage causes faster electron movement, producing a higher output current (Zhao et al., 2016).

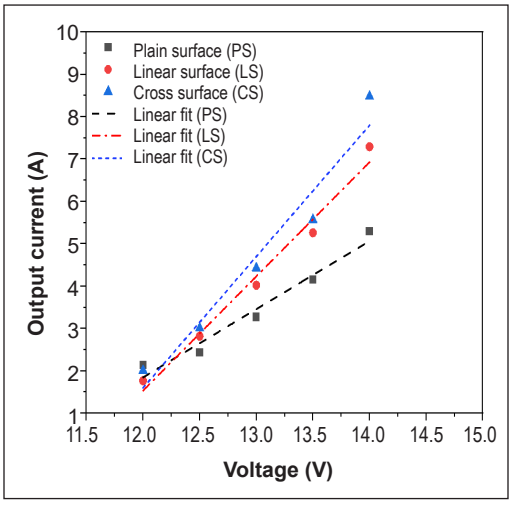

Figure 8. Applied voltage variations vs. output current under varying plate surface textures at 30g/L catalyst concentration

Effect of Applied Voltage on HHO Production Rate at Varying Plate Surface Textures

Figure 9 shows the HHO gas production as a function of applied voltage with variations in electrode surface texture. The results showed a significant increase in the HH gas production rate on the electrodes with linear and cross textures, namely 508.74 L/min and 573.82 L/min, respectively. A striking difference is seen for electrodes with plain surfaces, where the HHO gas rate is only 147.66 L/min. The increased applied voltage resulted in a uniform increase in charge density, promoting the acceleration of chemical reaction rates on the electrode surface by ion exchange (Lin et al., 2012). It is clearly seen that electrodes with textured surfaces are more effective in accommodating the ion exchange process to increase the rate of kinetics of the decomposition reaction in water electrolysis, which in turn can increase the rate of HHO gas production. The highest R^2 value was 0.979, achieved by the electrode with a linear surface texture. Lastly, this is also supportive evidence that HHO gas production is more promising on

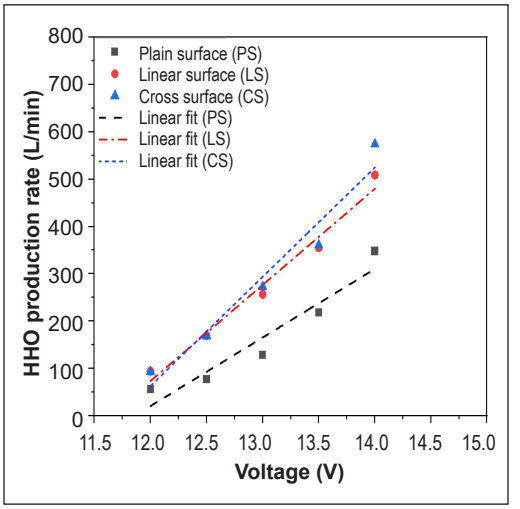

Figure 9. Applied voltage variations vs HHO production gas under varying plate surface textures at 30 g/L catalyst concentration

textured electrode surfaces. The results obtained are in accordance with the results stated by Mounir and Bellel (2011), where it is explained that the rate of hydrogen gas production will continue to increase as the voltage variation used increases.

Effect of Applied Voltage on Output Temperature at Varying Plate Surface Textures

Figure 10 shows various plate surface textures' applied voltage and output temperatures. At an applied voltage of 12 V, the resulting output temperature is 27.88°C for plain surfaces, 33.66°C for linear surfaces, and 32.71°C for cross surfaces. Interestingly, with increasing applied voltage, the output temperature increased slowly. At an input voltage of 14 V, the output temperature values achieved are 39.67°C for the plain surface, 37.52°C for the linear surface, and 44.11 °C for the cross surface. The increase in output temperature on the linear surface is the slowest compared to other electrode surfaces; the increase is only about 11.47% with an applied voltage range of 12 V–14 V. It seemed that increasing the input voltage had a lower impact on the output temperature at the linear surface compared with other surfaces. Increasing the output temperature may reduce the possibility of splitting water molecules. However, on the other hand, it can increase the reaction of the electrode surface and the ionic conductivity of electrolytes (El Kady et al., 2020). In addition, the accelerated mobility of ions due to increased applied voltage was also a reason for the increased output temperature.

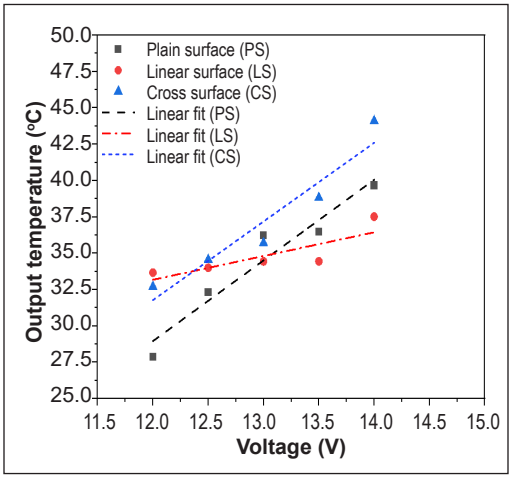

Figure 10. Applied voltage variations vs. output temperature under varying plate surface textures at 30 g/L catalyst concentration

CONCLUSION

The effect of varying NaOH electrolyte concentration in a range of 10 g/L to 60 g/L and electrode surface texture on the performance of the HHO generator was investigated. Several important points can be drawn from the present study as follows:

1. Overall, the output current, HHO gas production, and output temperature increase with increasing NaOH concentration and are also influenced by different electrode surface textures.
2. At a NaOH concentration of 60 g/L, the output currents on the linear and cross surfaces were 7.46 A and 9.95 A, respectively. Meanwhile, the HHO gas production for the linear and cross surfaces was 219.08 L/min and 305.93 L/min, respectively.

However, in terms of R2 value, the linear surface is better than the cross surface, where the R2 value is greater than 0.991 for both the output current and HHO gas production on the linear surface.

3. Additionally, the output temperature of the linear surface (i.e., 45.12 °C) was slightly lower than that of the cross surface (i.e., 46.55 °C) at a NaOH concentration of 60 g/L.
4. Similar to the NaOH concentration increment, the output current, HHO gas production, and output temperature also increased linearly with increasing applied voltage at varying electrode surface textures and a constant NaOH concentration of 30 g/L.
5. The HHO gas production on the linear surface and cross surface increased drastically at an output voltage of 14 V, to be about 508.74 L/min and 573.82 L/min, respectively. However, the R^2 value of the linear surface is higher than that of the cross surface, which is 0.979 and 0.955, respectively.

ACKNOWLEDGEMENT

The authors thank Universiti Teknikal Malaysia Melaka, as well as Universitas Nasional, Indonesia, for the financial support they provided throughout the completion of this study.

REFERENCES

Alam, N., & Pandey, K. M. (2017). Experimental Study of hydroxy gas (HHO) production with variation in current, voltage and electrolyte concentration. *IOP Conference Series: Materials Science and Engineering*, *225*(1), Article 012197. https://doi.org/10.1088/1757-899X/225/1/012197

Ayub, M. S., Yusof, S. N. A., Mohamed, S. B., Said, M. S., Asako, Y., Sidik, N. A. C., Kashim, M. S., & Mohamad, A. T. (2022). Effect of electrode plates on the engine performance and gas emissions of a four-stroke petrol engine. *Journal of Advanced Research in Fluid Mechanics and Thermal Sciences*, *90*(2), 90–108. https://doi.org/10.37934/arfmts.90.2.90108

Borghi, A., Gualtieri, E., Marchetto, D., Moretti, L., & Valeri, S. (2008). Tribological effects of surface texturing on nitriding steel for high-performance engine applications. *Wear*, *265*(7), 1046–1051. https://doi.org/10.1016/j.wear.2008.02.011

Cao, X. D., Kim, B. H., & Chu, C. N. (2009). Micro-structuring of glass with features less than 100μm by electrochemical discharge machining. *Precision Engineering*, *33*(4), 459–465. https://doi.org/10.1016/j.precisioneng.2009.01.001

Dincer, I., & Zamfirescu, C. (2012). Sustainable hydrogen production options and the role of IAHE. *International Journal of Hydrogen Energy*, *37*(21), 16266–16286. https://doi.org/10.1016/j.ijhydene.2012.02.133

Doche, M. L., Rameau, J. J., Durand, R., & Novel-Cattin, F. (1999). Electrochemical behaviour of aluminium in concentrated NaOH solutions. *Corrosion Science*, *41*(4), 805–826. https://doi.org/10.1016/S0010-938X(98)00107-3

Dufour, J., Serrano, D. P., Gálvez, J. L., Moreno, J., & González, A. (2011). Hydrogen production from fossil fuels: life cycle assessment of technologies with low greenhouse gas emissions. *Energy & Fuels*, *25*(5), 2194–2202. https://doi.org/10.1021/ef200124d

El Kady, M. A., Farrag, A. E. F., Gad, M. S., El Soly, A. K., & Abu Hashish, H. M. (2020). Parametric study and experimental investigation of hydroxy (HHO) production using dry cell. *Fuel*, *282*, Article 118825. /https://doi.org/10.1016/j.fuel.2020.118825

El Soly, A. K., El Kady, M. A., Farrag, A. E. F., & Gad, M. S. (2021). Comparative experimental investigation of oxyhydrogen (HHO) production rate using dry and wet cells. *International Journal of Hydrogen Energy*, *46*(24), 12639–12653. https://doi.org/10.1016/j.ijhydene.2021.01.110

Fahy, K. F. (2014). Enhancement of water electrolyzer efficiency. *Journal of Energy Technologies and Policy*, *4*(11), 1–2.

Fiala, J., Kuracina, M., Hrušovský, I., & Soldan, M. (2013). Study of basic characteristics of hydrogen generator. *Applied Mechanics and Materials*, *448–453*, 3078–3081. https://doi.org/10.4028/www.scientific.net/AMM.448-453.3078

Galama, A. H., Hoog, N. A., & Yntema, D. R. (2016). Method for determining ion exchange membrane resistance for electrodialysis systems. *Desalination*, *380*, 1–11. https://doi.org/10.1016/j.desal.2015.11.018

Grigoriev, S. A., Fateev, V. N., Bessarabov, D. G., & Millet, P. (2020). Current status, research trends, and challenges in water electrolysis science and technology. *International Journal of Hydrogen Energy*, *45*(49), 26036–26058. https://doi.org/10.1016/j.ijhydene.2020.03.109

Hassan, H., Aissa, W. A., Eissa, M. S., & Abdel-Mohsen, H. S. (2022). Enhancement of the performance and emissions reduction of a hydroxygen-blended gasoline engine using different catalysts. *Applied Energy*, *326*, Article 119979. https://doi.org/10.1016/j.apenergy.2022.119979

Ismail, T. M., Ramzy, K., Abelwhab, M. N., Elnaghi, B. E., El-Salam, M. A., & Ismail, M. I. (2018). Performance of hybrid compression ignition engine using hydroxy (HHO) from dry cell. *Energy Conversion and Management*, *155*, 287–300. https://doi.org/10.1016/j.enconman.2017.10.076

Karthik, N. B. V. S. R. (2017). Better performance of vehicles using HHO gas. *American Journal of Mechanical Engineering*, *5*(4), 167–174. https://doi.org/10.12691/ajme-5-4-9

Kato, H., Eyre, T. S., & Ralph, B. (1994). Sliding wear characteristics of nitrided steels. *Surface Engineering*, *10*(1), 65–74. https://doi.org/10.1179/sur.1994.10.1.65

Li, H., Xu, W., Li, L., Xia, H., Chen, X., Chen, B., Song, X., & Tan, C. (2022). Enhancing the wettability for 4043 aluminum alloy on 301L stainless steel via chemical-etched surface texturing. *Journal of Materials Processing Technology*, *305*, Article 117577. https://doi.org/10.1016/j.jmatprotec.2022.117577

Li, Z., Bai, J., & Tang, J. (2018). Micro-EDM method to fabricate three-dimensional surface textures used as SERS-active substrate. *Applied Surface Science*, *458*, 810–818. https://doi.org/10.1016/j.apsusc.2018.07.132

Lin, M. Y., Hourng, L. W., & Kuo, C. W. (2012). The effect of magnetic force on hydrogen production efficiency in water electrolysis. *International Journal of Hydrogen Energy*, *37*(2), 1311–1320. https://doi.org/10.1016/j.ijhydene.2011.10.024

Manu, P. V., Sunil, A., & Jayaraj, S. (2016). Experimental investigation using an on-board dry cell electrolyzer in a CI engine working on dual fuel mode. *Energy Procedia*, *90*, 209–216. https://doi.org/10.1016/j.egypro.2016.11.187

Mazloomi, S. K., & Sulaiman, N. (2012). Influencing factors of water electrolysis electrical efficiency. *Renewable and Sustainable Energy Reviews*, *16*(6), 4257–4263. https://doi.org/10.1016/j.rser.2012.03.052

Mounir, S., & Bellel, N. (2011). Hydrogen production by electrolysis of brine using a source of renewable energy. *International Review of PHYSICS*, *5*(4), 158–161.

Muritala, I. K., Guban, D., Roeb, M., & Sattler, C. (2020). High temperature production of hydrogen: Assessment of non-renewable resources technologies and emerging trends. *International Journal of Hydrogen Energy*, *45*(49), 26022–26035. https://doi.org/10.1016/j.ijhydene.2019.08.154

Naat, N., Boutar, Y., Naïmi, S., Mezlini, S., & Da Silva, L. F. M. (2023). Effect of surface texture on the mechanical performance of bonded joints: A review. *The Journal of Adhesion*, *99*(2), 166–258. https://doi.org/10.1080/00218464.2021.2008370

Olivares-Ramírez, J. M., Campos-Cornelio, M. L., Uribe Godínez, J., Borja-Arco, E., & Castellanos, R. H. (2007). Studies on the hydrogen evolution reaction on different stainless steels. *International Journal of Hydrogen Energy*, *32*(15), 3170–3173. https://doi.org/10.1016/j.ijhydene.2006.03.017

Poimenidis, I. A., Tsanakas, M. D., Papakosta, N., Klini, A., Farsari, M., Moustaizis, S. D., & Loukakos, P. A. (2021). Enhanced hydrogen production through alkaline electrolysis using laser-nanostructured nickel electrodes. *International Journal of Hydrogen Energy*, *46*(75), 37162–37173. https://doi.org/10.1016/j.ijhydene.2021.09.010

Rajput, H., Atulkar, A., & Porwal, R. (2021). Optimization of the surface texture on piston ring in four-stroke IC engine. *Materials Today: Proceedings*, *44*(1), 428–433. https://doi.org/10.1016/j.matpr.2020.09.752

Rao, X., Sheng, C., Guo, Z., Zhang, X., Yin, H., Xu, C., & Yuan, C. (2021). Effects of textured cylinder liner piston ring on performances of diesel engine under hot engine tests. *Renewable and Sustainable Energy Reviews*, *146*, Article 111193. https://doi.org/10.1016/j.rser.2021.111193

Ridhuan, A., Osman, S. A., Fawzi, M., Alimin, A. J., & Osman, S. A. (2021). A review of comparative study on the effect of hydroxyl gas in internal combustion engine (ICE) on engine performance and exhaust emission. *Journal of Advanced Research in Fluid Mechanics and Thermal Sciences*, *87*(2), 1–16. https://doi.org/10.37934/arfmts.87.2.116

Rusdianasari, Bow, Y., & Dewi, T. (2019). HHO gas generation in hydrogen generator using electrolysis. *IOP Conference Series: Earth and Environmental Science*, *258*(1), Article 012007. https://doi.org/10.1088/1755-1315/258/1/012007

Santilli, R. M. (2006). A new gaseous and combustible form of water. *International Journal of Hydrogen Energy*, *31*(9), 1113–1128. https://doi.org/10.1016/j.ijhydene.2005.11.006

Soler, L., Candela, A. M., Macanás, J., Muñoz, M., & Casado, J. (2009). In situ generation of hydrogen from water by aluminum corrosion in solutions of sodium aluminate. *Journal of Power Sources*, *192*(1), 21–26. https://doi.org/10.1016/j.jpowsour.2008.11.009

Subramanian, B., & Thangavel, V. (2020). Analysis of onsite HHO gas generation system. *International Journal of Hydrogen Energy*, *45*(28), 14218–14231. https://doi.org/10.1016/j.ijhydene.2020.03.159

Sun, C. W., & Hsiau, S. S. (2018). Effect of electrolyte concentration difference on hydrogen production during pem electrolysis. *Journal of Electrochemical Science and Technology*, *9*(2), 99–108. https://doi.org/10.5229/JECST.2018.9.2.99

Vračar, L., & Conway, B. E. (1990). Hydride formation at Ni-containing glassy-metal electrodes during the H_2 evolution reaction in alkaline solutions. *Journal of Electroanalytical Chemistry and Interfacial Electrochemistry*, *277*(1), 253–275. https://doi.org/10.1016/0022-0728(90)85106-F

Wang, S., Lu, A., & Zhong, C. J. (2021). Hydrogen production from water electrolysis: Role of catalysts. *Nano Convergence*, *8*(1), 1-23. https://doi.org/10.1186/s40580-021-00254-x

Xu, Y., Wang, C., Huang, Y., & Fu, J. (2021). Recent advances in electrocatalysts for neutral and large-current-density water electrolysis. *Nano Energy*, *80*, Article 105545. https://doi.org/10.1016/j.nanoen.2020.105545

Yilmaz, A. C., Uludamar, E., & Aydin, K. (2010). Effect of hydroxy (HHO) gas addition on performance and exhaust emissions in compression ignition engines. *International Journal of Hydrogen Energy*, *35*(20), 11366–11372. https://doi.org/10.1016/j.ijhydene.2010.07.040

Yuvaraj, A. L., & Santhanaraj, D. (2014). A systematic study on electrolytic production of hydrogen gas by using graphite as electrode. *Materials Research*, *17*(1), 83–87. https://doi.org/10.1590/S1516-14392013005000153

Zeng, K., & Zhang, D. (2010). Recent progress in alkaline water electrolysis for hydrogen production and applications. *Progress in Energy and Combustion Science*, *36*(3), 307–326. https://doi.org/10.1016/j.pecs.2009.11.002

Zeng, K., & Zhang, D. (2014). Evaluating the effect of surface modifications on Ni based electrodes for alkaline water electrolysis. *Fuel*, *116*, 692–698. https://doi.org/10.1016/j.fuel.2013.08.070

Zhao, Z., Zhang, Y., Quan, X., & Zhao, H. (2016). Evaluation on direct interspecies electron transfer in anaerobic sludge digestion of microbial electrolysis cell. *Bioresource Technology*, *200*, 235–244. https://doi.org/10.1016/j.biortech.2015.10.021